Kumar et al. Renewables (2017) 4:2
DOI 10.1186/s40807-017-0039-7

Renewables: Wind, Water, and Solar

ORIGINAL RESEARCH ARTICLE

Open Access

# Sensitivity analysis-based performance and economic operation of wind-integrated system with FACTS devices for optimum load dispatch

Satish Kumar[1,2*], Ashwani Kumar[1] and Nikhlesh Kumar Sharma[3]

**Abstract**

Supply of additional power generation by wind system to increase total power generation is increasing exponentially and globally to meet the challenge of surplus power demand. This total power generation should be at minimum cost and power loss, without violating stability limits. This paper presents modelling and tuning of flexible A.C. Transmission system (FACTS) devices with sensitivity analysis of buses for wind-integrated system (WIS). When the conventional grid system is integrated with some renewable energy resources such as wind, the voltage of buses within the system tends to decrease. This dip in voltage profile of the system must be compensated by some suitable FACTS devices, which must be optimally placed so as to improve the voltage and current profile of the system. Particle swarm optimization algorithm is used here for suitable placement and precise tuning of FACTS devices to maintain the voltage profile of integrated system within stability limits. Optimal power flow (OPF) is also used in this paper to maintain steady-state operation of wind integrated system with mitigation of cost of generation and losses. OPF is computed and compared with and without placing FACTS devices for WIS. Total per unit generation cost and losses are also calculated and compared for FACTS-controlled WIS. Bus voltage and angle sensitivity have been calculated and presented to determine range of voltage stability and to prevent any possible voltage collapse or critical point within the system. Optimization of load between maxima and minima is solved using general algebraic modelling system software.

**Keywords:** Wind integration, FACTS, Cost function, Voltage stability, Senstivity , PF, CPF, OPF, Voltage collapse, PSO

## Background

Exponential increase in power demand by variety of applications has compelled the power researchers to increase in power generation from conventional as well as from renewable energy resources. But due to increase in power generation, cost of power generation and losses also increases because of increase in cost of fuel consumed, installation cost and various losses incurred during the generation, transmission and distribution due to the distributed parameters present in the system. This increase in power generation may cause variations in voltage limits, thermal limits or possibility of voltage collapse at different stages of generation or transmission due to variable loading conditions at the consumers end. So it is highly desirable to synchronize this variation in load with the voltage profile of the integrated system. In recent years, renewable energy resources such as solar energy, wind energy, hydropower, geothermal energy and biomass energy have achieved significant contribution to support this surplus power in addition to the conventional power sources, so as to increase total power generation by the plant. WIS is most common and fastest growing application of power generation (Chi et al. 2006). Electricity produced from the wind systems differs from conventional methods only because of the power flow between wind energy system and transmission grid depends on fluctuating wind speed (Joslin Hurbert et al.

*Correspondence: Satish_1298-10@nitkkr.ac.in
[1] Department of Electrical Engineering, National Institute of Technology (NIT), Kurukshetra, Haryana 136119, India
Full list of author information is available at the end of the article

2007). Three types of commercial wind turbines systems have also been developed and integrated with conventional grid system to generate more cost-effective power. It is also seen that sites can be more profitable for electrical and mechanical applications, i.e. water pumping and battery charging, if planned properly (Gaddada and Kodicherla 2016). Wind integration with conventional grid system can be made smooth and cost-effective by incorporating adequate control strategies in the multimachine system. The implementation of optimal controllers is one of the ways which not only offer good dynamic performance, but ensure system dynamic stability also (Ehtesham et al. 2016).

Optimal power flow (OPF) is very useful tool to meet the challenge of variable wind speed, for wind-integrated system especially if we consider the economic operation of power generating units (Segura et al. 2011; Momoh 1989). Main purpose of implementing OPF is to minimize the total cost of generation by power balance at each node using power flow equations with inequality constraints, i.e. network operating limits (line flows, voltages) and limits on control variables. So evaluation of OPF is very necessary and valuable specially when integration of wind energy system with conventional systems is incorporated to meet the variable load and increased power demand of consumer. It is also preferred to maintaining the voltage stability of the integrated system within the prescribed limit (Momoh et al. 1997). Another approach of power flow (PF), called continuation power flow (CPF), should also remain well conditioned at and around the critical point within the system (Ajjarapu and Christy 1998). So power flow solutions starting from some base load to full load should be carried out to maintain voltage stability limit for WIS. Previously various voltage problems on transmission networks subject to unusual power flow patterns have been identified which has compelled the power engineers to go for optimal power flow solutions to meet the challenges (Ilic and Stankovic 1991). Line stability indices-based method is also valuable for calculating voltage stability limits and for monitoring voltage regulations in the multimachine-integrated systems for better planning and estimation (Lof et al. 1992). Earlier OPF was applied only with thermal energy power sources, but now due to increased demand and recent developments in renewable energy resources, inclusion of generating cost of wind energy system units has also become mandatory in classical OPF problem (Shi et al. 2012; Hetzer et al. 2008).

FACTS are power electronic devices which are frequently used to resolve and maintain various types of stability problems in power system planning and operation. Very common types of FACTS are shunt devices such as static VAR compensators (SVC) and series devices such as thyristor-controlled series compensators (TCSC), which in combination with wind energy system can boost the generated power (Jovcic and Pillai 2005).

Estimation of power generation with integration of wind energy system by tuning power devices using optimization techniques is important but rigorous (Momoh 2001; Wood and Wollenberg 1996). But evolutionary programming-based OPF algorithm is user-friendly and well suited for problem solving (Yuryevich and Wong 1999).

MATPOWER tool box is available in the MATLAB and can be used for the power flow and optimal power flow calculations for WIS because it gives direct results for power flow in terms of bus voltages and angles (Zimmerman et al. 2007). Various optimization techniques such as particle swarm optimization (PSO), genetic algorithm (GA) or artificial neural network (ANN) are available for optimizing cost function of system integrated with renewable energy resources. It is observed that finding solution using PSO is advantageous over GA, as it does not have evolution operators such as crossover and mutation (Mo et al. 2007). In PSO, particles update themselves with the internal velocity as they also have memory, which is important to the algorithm. PSO is also useful to integrate and locate FACTS devices when load on the system is uncertain and fluctuating in nature. Placement of FACTS devices within the system is mainly done to improve the voltage profile of the system, system loadability and minimization of losses. System performance analysis using GA and PSO (Shakib et al. 2009) shows that PSO gives better placement of FACTS devices to increase availability of power at users end. Variable speed wind turbines equipped with doubly fed induction generator (DFIG) are also widely used for advanced reactive power and voltage control strategies for wind-integrated systems (Shi et al. 2012).

## Organization of paper

The organization of paper is as follows: Background section explains the basic philosophy and motivation of work done in the area of voltage stability, optimization and power flow techniques. The importance of integrating wind energy systems with FACTS devices along with the need for optimal placement of FACTS devices is also presented. Optimal Power Flow with Wind Power Integration section explains the method to solve optimal power flow (OPF) for wind integrated system with necessary and governing equations. Particle Swarm Optimization Technique (PSO) explains the need of implementing PSO with its advantages over other intelligent techniques. Section Objective Function Formulation suggests formulation of objective function with and without integration of wind system with modelling of FACTS devices for optimal power flow to meet the variable load demand at the users end. Modelling of SVC and TCSC Using Firing Angle Control section presents N-R power flow solution in terms of firing angle. In Bus Voltage and Angle Sensitivity Analysis section, branch and bus sensitivities of IEEE-14 bus wind integrated system have been calculated to determine OPF. Similarly, procedure to find voltage stability index for maximum loading condition is presented in Determination of Voltage Stability Index (VSI). All concrete results and their detailed explanation with and without wind integrated system and performance of FACTS devices are presented in Results and Discussion section followed by Conclusion in which the usefulness of the software like GAMS and the work done is presented.

## Optimal power flow with wind power integration

The basic purpose to run OPF is to solve control variable in the objective function so as to minimize the installation cost of generators, with and without wind integration considering system design and operation. With the application of PSO, OPF is solved for control variables of objective function. Based on objective function with and without wind integration new position and velocity gets updated to give the best result. Relation between wind speed and aerodynamics torque of WIS is given by,

$$P_{\mathrm{w}} = \frac{1}{2}\rho\pi R^2 V_{\mathrm{w}}^3 C_{\mathrm{p}}(\Theta, \lambda_{\mathrm{w}}) \tag{1}$$

$$T_{\mathrm{w}} = \frac{1}{2}\rho\pi R^3 V_{\mathrm{w}}^2 C_{\mathrm{p}}(\Theta, \lambda_{\mathrm{w}})/\lambda_{\mathrm{w}}. \tag{2}$$

## Particle swarm optimization technique (PSO)

To solve optimization problem some well-established computational programming techniques are available such as GA and evolutionary programming (EP). These techniques have been successfully implemented to solve some complex problems accurately and effectively (Gerbex et al. 2001; Venkatesh et al. 2003). PSO is a robust stochastic optimization technique based on the movement and intelligence of swarms which was developed in 1995 by James Kennedy (Social Psychologist) and Russell Eberhard (Electrical Engineer). PSO uses a number of agents (particles) that constitute a swarm moving around in the search space looking for the best solution. General procedure to implement PSO is defined in many literature which are using optimization techniques for finding optimum solution (Saravanan et al. 2007) which show advantages of PSO ($G_{\mathrm{best}}$ model) over other intelligent techniques. PSO evaluates the objective function at each particle location and determine the best (lowest) function value and the best location. It chooses new velocities based on current velocities, the particle individual best locations and the best locations of the neighbours (new location is the old location plus one). Iteration proceeds until the algorithm reaches a stopping criteria. PSO is advantages as,

- PSO is easy to implement and needs only few parameters to adjust.
- Ability to find global optima and optimal power flow.
- Non-gradient and derivative-free method (Prasanthi and Sindhu 2014; Al Rashidi et al. 2010).

To find the optimize solution, location of FACTS devices, their setting (tuning), their type (series or shunt) and installation cost of FACTS devices are chosen as parameters of PSO. The variables for the optimization for each device are its location in the network, its setting and the installation cost. The location of FACTS devices is also calculated using PSO. Installation of FACTS devices have been done only at identified weak buses.

## Objective function formulation

Objective function to determine optimal power flow solution for IEEE 14 bus wind-integrated system can be written as,

$$\mathrm{Function}\left(P_{\mathrm{gn}}, P_{\mathrm{gw}}, t\right) = \sum_{n=1}^{N_{\mathrm{g}}} C_n\left(P_{\mathrm{gn}}\right) + \sum_{s=1}^{N_{\mathrm{c}}} C_{\mathrm{w}}\left(P_{\mathrm{gw}}^t\right) \tag{3}$$

Subject to,

$$P_{\mathrm{gn}} + \sum_{s=1}^{N_{\mathrm{w}}}\left(P_{\mathrm{gw}}^{\max}\right) = \sum_{j=1}^{N_{\mathrm{L}}} P_{\mathrm{di}} \tag{4}$$

$$C_{\mathrm{gn}}\left(P_{\mathrm{gn}}\right) = a_n P_{\mathrm{gn}}^2 + b_n P_{\mathrm{gn}} + c_n \tag{5}$$

$a_n$, $b_n$ and $c_n$ are the cost coefficient of $n$ no. of units.

To minimize active power generation cost of wind-integrated system is to placing FACTS devices optimally, Considering the total load demand of 850 MW, this objective function is to be minimized for each PV Bus, except slack bus, such that $150 < f(n) < 850$.

The constraints are,

$$P_{\mathrm{gn}}^{\mathrm{Min}} \le P_{\mathrm{gn}} \le P_{\mathrm{gn}}^{\mathrm{Max}}, \quad n = 1 \dots T_{\mathrm{g}} \tag{6}$$

$$Q_{\mathrm{gn}}^{\mathrm{Min}} \le Q_{\mathrm{gn}} \le Q_{\mathrm{gn}}^{\mathrm{Max}}, \quad n = 1 \dots T_{\mathrm{g}} \tag{7}$$

$$V_n^{\mathrm{Min}} \le V_n \le V_n^{\mathrm{Max}}, \quad n = 1 \dots T_{\mathrm{b}} \tag{8}$$

Optimal placement of FACTS devices to minimize the cost of installation of FACTS devices is given by

$$\text{Minimize} \quad \mathbf{IC_{FACTS}} = C \times S \times 1000 \tag{9}$$

IC is the optimal installation cost of FACTS devices in US$
$C$ is the cost of installation of FACTS devices in US$/KVAR
$S$ is the operating range of FACTS devices in MVAR

$$S = |Q_n| - |Q_{n-1}| \tag{10}$$

The cost function of SVC, TCSC and UPFC is given by Sharma et al. (2016),

$$c_{SVC} = 0.0003s^2 - 0.3051s + 127.38 \text{ (US\$/Kvar)} \tag{11}$$

$$c_{TCSC} = 0.0015s^2 - 0.7130s + 153.75 \text{ (US\$/Kvar)} \tag{12}$$

$$c_{UPFC} = 0.0003s^2 - 0.2691s + 189.22 \text{ (US\$/Kvar)} \tag{13}$$

## Initial conditions

To solve OPF, the initial conditions for all node voltage is assumed as 1.0 per unit, with phase angle of $10^0$ for all buses and starting firing angle of $10^0$ for both TCSC and SVC.

## Modelling of SVC using firing angle control

$$Q_k = \frac{-V_{k^2}}{X_C X_L}\left\{X_L - \frac{X_C}{\pi}[2(\pi - \alpha_{SVC}) + \text{Sin}(2\alpha_{SVC})]\right. \tag{14}$$

Static VAR compensator equation in linear form, so as to compute in the cost function can be written as,

$$\begin{bmatrix}\dfrac{\Delta P_k}{\Delta Q_k}\end{bmatrix}^{(i)} = \begin{bmatrix} 0 & 0 \\ 0 & \frac{2V_k^2}{\pi X_C}[\text{Cos}(2\alpha_{SVC}) - 1] \end{bmatrix}^{(i)} \begin{bmatrix}\dfrac{\Delta Q_k}{\Delta \alpha_{SVC}}\end{bmatrix}^{(i)} \tag{15}$$

After $i$th iteration the firing angle $\alpha$ is updated every time to maintain the bus voltage magnitude equal to 1 per unit. So modified value of firing angle after $i$th iteration can be given by,

$$\alpha_{SVC}^{(i)} = \alpha_{SVC}^{(i-1)} + \Delta\alpha_{SVC}^{(i)}. \tag{16}$$

## Modelling of TCSC using firing angle control

Two power flow models are available to study the impact of TCSC. The easier one is called variable series reactance, which is automatically adjustable in nature to satisfy the demand of active power flow through it. The advance model called firing modal uses directly the firing angle characteristics, which is nonlinear in nature, so for power flow solutions α is chosen as static variable in N–R power flow solutions.

Active and reactive power at bus $i$ are given as,

$$P_i = V_i V_j B_{ij} \text{Sin}(\Theta_i - \Theta_j) \tag{17}$$

$$Q_i = -V_i^2 B_{ii} - V_i V_j B_{ij} \cos(\theta_i - \theta_j) \tag{18}$$

where $B_{ij} = \frac{1}{X_{TCSC}} = B_{ji}$ and $B_{ii} = -\frac{1}{X_{TCSC}} = B_{jj}$.

N–R solution converges to the point when Eqs. (4)–(8) are expressed in linear form up to the point $P_{ij}^{\text{Linear}}$.

Hence, we can write,

$$\Delta P_{ij}^{X_{TCSC}} = \Delta P_{ij}^{\text{Linear}} - \Delta P_{ij}^{\text{Linear Actual}}. \tag{19}$$

Similarly change in reactance is given by,

$$\Delta X_{TCSC}^i = X_{TCSC}^i - X_{TCSC}^{i-1} \tag{20}$$

$X_{TCSC}$ is updated at the end of each iterations, so

$$X_{TCSC}^i = X_{TCSC}^{i-1} + \left(\frac{\Delta X_{TCSC}}{X_{TCSC}}\right)^i X_{TCSC}^{(i-1)}. \tag{21}$$

## Bus voltage and angle sensitivity analysis

Voltage stability analysis in large complex power system is done to obtain the critical point in the system, but this critical point also gets affected when system conditions are changed. Identification of system stability index is done with the analysis of system sensitivity. The influence of voltage profile, angle profile, active power, reactive power and momentarily change in these parameters is calculated for better planning of the system and to prevent instability in the system. So bus sensitivity indicates how a particular bus is near the critical point and how much bus is close to bus voltage instability.

For optimal power flow, branch and bus sensitivity for IEEE 14 bus wind-integrated system can be calculated. So bus sensitivity in terms of bus voltage magnitude can be given by,

$$\frac{\mathrm{d}h}{\mathrm{d}\lambda} = \sum_{j=1}^{n} \frac{\partial V_i}{\partial x_i}.\frac{\mathrm{d}x_j}{\mathrm{d}\lambda} + \frac{\partial V_i}{\partial \lambda} \tag{22}$$

$$\begin{aligned} &= \frac{\partial V_i}{\partial V_i}.\frac{\mathrm{d}V_i}{\mathrm{d}\lambda} + 0 \\ &= \frac{\partial V_i}{d\lambda} \end{aligned}. \tag{23}$$

If we consider bus voltage angle, then sensitivity in terms of voltage angle senstivity can be given by,

$$\frac{\mathrm{d}h}{\mathrm{d}\lambda} = \frac{\partial \delta_i}{d\lambda}. \tag{24}$$

## Determination of voltage stability index (VSI)

Researchers have already used the derivation of voltage stability index is Reis and Maciel Barbosa (2009). One way to find weakest bus in the system is $d$ from the maximum drop in the reactive power of the bus ($V_i$) with

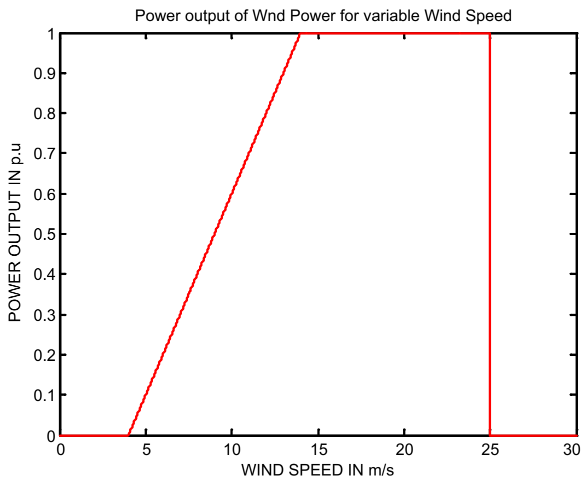


**Fig. 1** Wind power output for different wind speed (m/s)

available maximum load ($P_{\text{total}}$). If the differential change in the load is $\frac{dV_i}{dP_{\text{total}}}$, the weakest bus is represented by,

$$\left|\frac{dV_j}{d\lambda}\right| = \text{Max}\left\{\left|\frac{dV_1}{d\lambda}\right|, \left|\frac{dV_2}{d\lambda}\right|, \ldots, \left|\frac{dV_n}{d\lambda}\right|\right\}. \quad (25)$$

Voltage stability index in terms of minimum real part of eigenvalue and minimum singular value of Jacobian is defined (Musirin et al. 2002). The tangent vector is right eigenvector of the Jacobian corresponding to zero eigenvalue at critical (voltage collapse) point

## Results and discussion

Power output of wind system integrated with IEEE 14 bus system for different wind speed is shown in Fig. 1. IEEE 14 bus system simulated on power system analysis Simulink library is shown in Fig. 2. Figure 1 shows that the wind power output increases linearly from 3.8 to 12 m/s and reaches to maximum of 1 p.u. The power output remains constant for a wind speed of 12–25 m/s and comes down to zero output, if wind speed increases beyond 25 m/s for the system under study. Objective function is formulated for this wind-integrated system to minimize total cost of generation and losses and is solved using GAMS for minimum and maximum loading condition. The objective function before and after minimization is presented in Figs. 3 and 4, respectively, which shows that the condition of maxima and minima load is achieved for WIS. Sensitivity analysis of voltages for weak buses of WIS is shown in Figs. 5 and 6 respectively. Figure 7 presents variation in voltage stability index for maximum load of 850 MW, with discrete values of sensitivity index for different loads. It is also clear from Fig. 7 that for a total generation of 850 MW by wind integrated system, the maximum and minimum power generation is found to be 393.30 and 122.2 MW with a total power loss of 78.44 MW including variable and fixed losses.

The bus voltages with magnitude and phase angle for this maximum and minimum power generation are presented in Tables 1 and 2 and Fig. 8, respectively. From the results, it is clear that for minimum power generation all the buses are within the voltage stability limits, but for maximum generation there is variation and imbalance of voltages in different buses of the WIS. Placement of SVC and TCSC is done optimally using PSO for identified weak buses in the WIS. OPF is terminated in five iterations using N–R Method, giving considerable decremental changes in power loss with SVC and TCSC for maximum and minimum load of 400–150 MW. Comparison of power loss with and without FACTS controllers for WIS is presented in Table 3 and Fig. 9 which shows that power loss is less using TCSC as compared to SVC. Further tuning of SVC and TCSC for WIS with firing angle control gives more voltage support to system for maintaining voltages of the weak buses and to maintain stability of the system within the limits. Power loss is further minimized up to 72.84 MW by tuning SVC with firing angle α from 138° to 130.6° and up to 72.39 MW by tuning TCSC with firing angle α from 141.68° to 123.90°. Compensation in power loss by both SVC and TCSC is approximately 0.45 MW for WIS, which is very significant power saving for a small system. Compensation in power loss can be increased further, if system considered is large with more series and shunt devices and fine tuning of firing angle control. TCSC is mainly used here to increase power transfer capability and to improve transient stability of the wind-integrated system. With the help of TCSC, fault current can also be limited while the voltage stability is also improved. So choice of SVC and TCSC within the system should be taken considering the economic aspects of the composite system. Table 4 presents the change in the voltage levels of the different buses for different firing angles (change in firing angle is very small and precise) obtained from tuning of SVC and TCSC for variable wind penetration level from 20 to 100%, though 100% wind penetration level is not possible practically all the time. Cost of power generation by WIS with and without using SVC and TCSC is given in Table 5 and shows that as the power generation level increases, the cost of power generation per hour also increases, but not very large due to the voltage support by the two FACTS devices placed suitably. Saving in cost of generation for base load to peak load with and without using SVC and TCSC and Voltage support by FACTS devices with firing angle control for different level of wind penetration is presented in Fig. 10. Both SVC and TCSC develop more voltage support by regulating firing angle of the circuit to maintain the voltage stability limit,

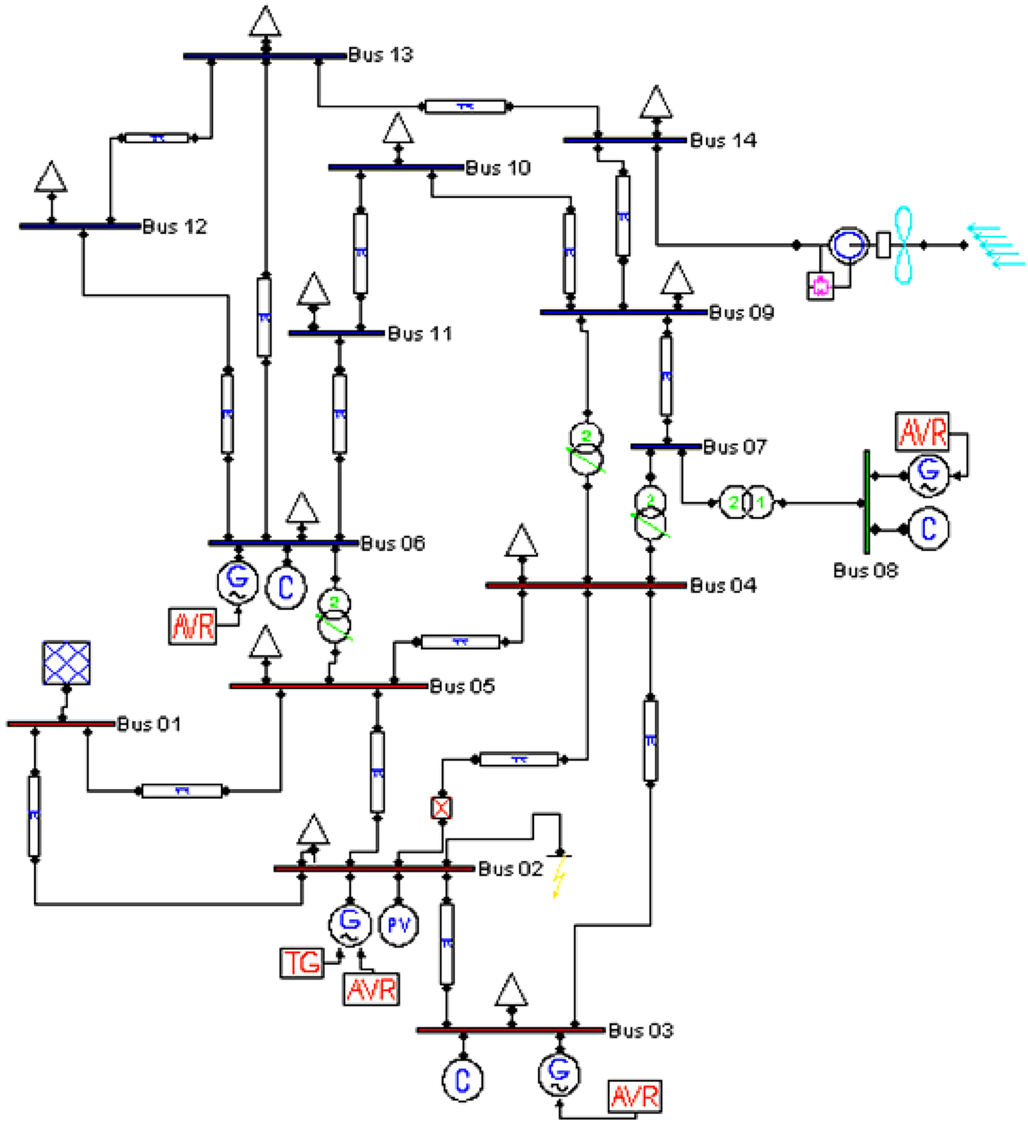


**Fig. 2** Wind-integrated 14 Bus multimachine system

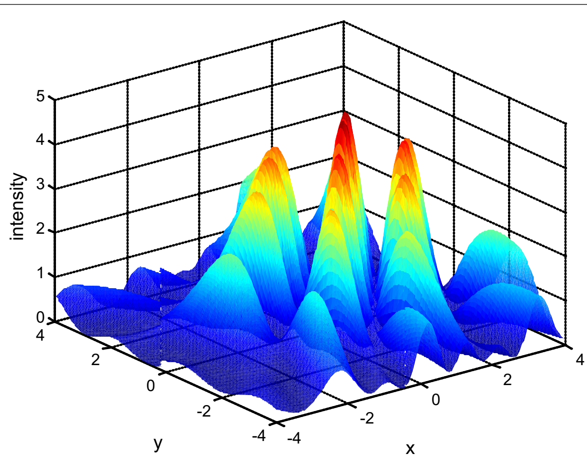


**Fig. 3** Non-minimize objective function with wind integration

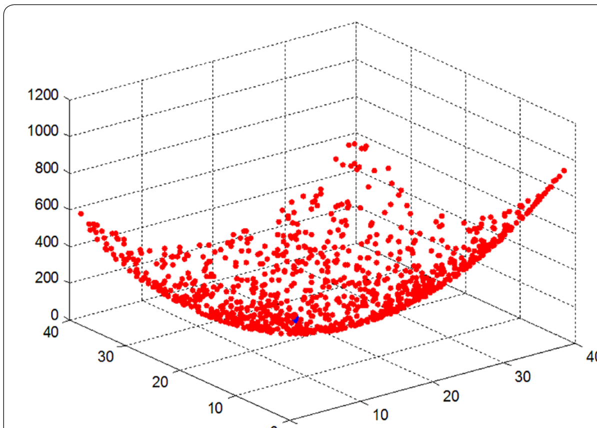

**Fig. 4** Minimized objective function with wind integration using PSO

**Table 1 Bus voltage angle- and magnitude-based sensitivity analysis for WIS**

| No. | Bus no. | Tangent vector for voltage angle | Voltage angle sensitivity $\frac{\partial \delta_i}{d\lambda}$ | Tangent vector for voltage magnitude ($V_i$) | Voltage mag. sensitivity $\frac{\partial V_i}{d\lambda}$ |
|---|---|---|---|---|---|
| 1 | 3 | 0.17206 | 1.0000 | 1.0000 | 1.0000 |
| 2 | 1 | 0.17119 | 0.9952 | −0.9981 | −0.9981 |
| 3 | 8 | 0.16209 | 0.9712 | −0.9669 | −0.9669 |
| 4 | 6 | 0.16113 | 0.9253 | −0.9571 | −0.9571 |
| 5 | 11 | 0.15792 | 0.8825 | −0.9333 | −0.9333 |
| 6 | 2 | 0.15348 | 0.8695 | −0.8997 | −0.8997 |
| 7 | 4 | 0.15111 | 0.8313 | −0.8649 | −0.8649 |
| 8 | 5 | 0.14881 | 0.7976 | −0.8412 | −0.8412 |
| 9 | 14 | 0.14628 | 0.7761 | −0.8111 | −0.8111 |
| 10 | 9 | 0.13667 | 0.7123 | −0.7939 | −0.7939 |
| 11 | 10 | 0.13419 | 0.6912 | −0.7775 | −0.7775 |
| 12 | 7 | 0.13291 | 0.6777 | −0.7558 | −0.7558 |
| 13 | 12 | 0.12825 | 0.6485 | −0.7113 | −0.7113 |
| 14 | 13 | 0.12344 | 0.6117 | −0.6999 | −0.6999 |

**Table 2 Bus voltage profile of different buses using OPF with wind integration**

| S. no. | Bus no. | Voltage (p.u.) at 334.6 MW | Voltage (p.u.) at 393.2 MW | Voltage (p.u.) at 122 MW |
|---|---|---|---|---|
| 1 | 1 | 1.029 | 1.026 | 1.129 |
| 2 | 2 | 1.021 | 1.018 | 1.126 |
| 3 | 3 | 0.929 | 0.911 | 1.119 |
| 4 | 4 | 0.978 | 0.926 | 1.136 |
| 5 | 5 | 1.018 | 1.006 | 0.998 |
| 6 | 6 | 0.999 | 0.976 | 1.001 |
| 7 | 7 | 0.952 | 0.949 | 0.936 |
| 8 | 8 | 1.002 | 0.998 | 0.882 |
| 9 | 9 | 1.039 | 1.027 | 1.019 |
| 10 | 10 | 0.983 | 0.973 | 0.896 |
| 11 | 11 | 0.958 | 0.951 | 0.889 |
| 12 | 12 | 0.939 | 0.883 | 0.891 |
| 13 | 13 | 0.926 | 0.913 | 0.875 |
| 14 | 14 | 0.911 | 0.913 | 0.866 |

but there is not much difference in the voltage levels of the buses no. 13 and 14, when the wind penetration level is increased from 75 to 100%. SVC being connected in series of the weak bus gives more voltage boost as compared to the shunt device, though TCSC gives more support to reduce power loss due to its ability to limit the fault current within the system.

## Conclusion

For wind-integrated system, N–R method is used to calculate power flow, i.e. voltage magnitude and angle at each bus of wind-integrated system by using power balance equations. Minimization of cost of generation including wind for economic operation of integrated system is solved using GAMS 23.4 software and is also explained and presented here. Simulations are performed on IEEE 14 bus wind-integrated system. PSO as one of the best computer intelligence techniques for solving optimization problem is applied both for placement of FACTS devices at suitable locations and to improve the system loadability. Power loss comparison with and without FACTS devices is also presented for simulated system using optimal power flow. SVC gives lowest cost of power generation as compared to TCSC, but system loadability is much more improved with the help of TCSC. Sensitivity analysis of buses for wind-integrated system is also

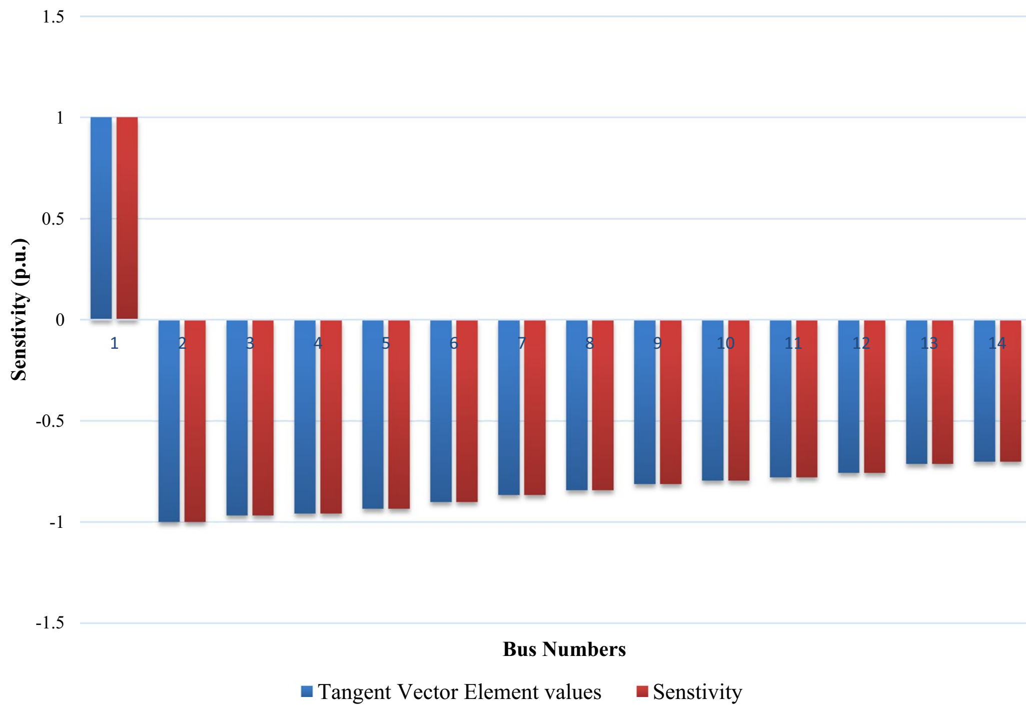


**Fig. 5** Voltage magnitude-based sensitivity profile for WIS

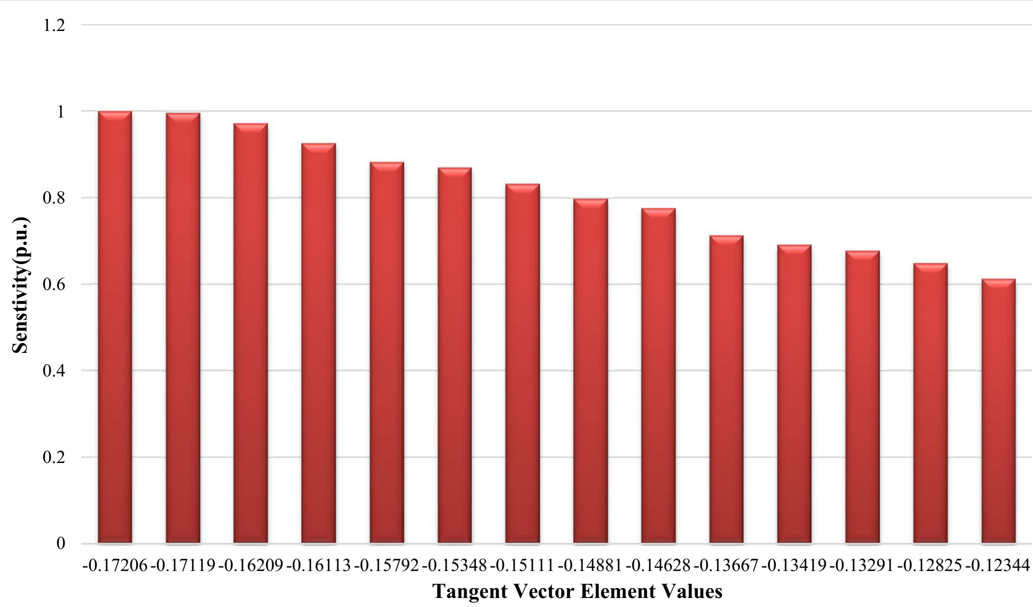


**Fig. 6** Voltage angle-based sensitivity profile for WIS

performed which provides the possibility of voltage collapse within the system and for proximity of the fault for identified weak buses within the wind-integrated system so as to place FACTS devices at the point of possible fault for necessary and corrective voltage support to increase available power.

## Abbreviations

WIS: wind-integrated system; PSO: particle swarm optimization; FACTS: flexible AC transmission; OPF: optimal power flow; PF: power flow; CPF: continuous power flow; SVC: static VAR compensator; TCSC: thyristor-controlled series compensation; GA: genetic algorithm; ANN:

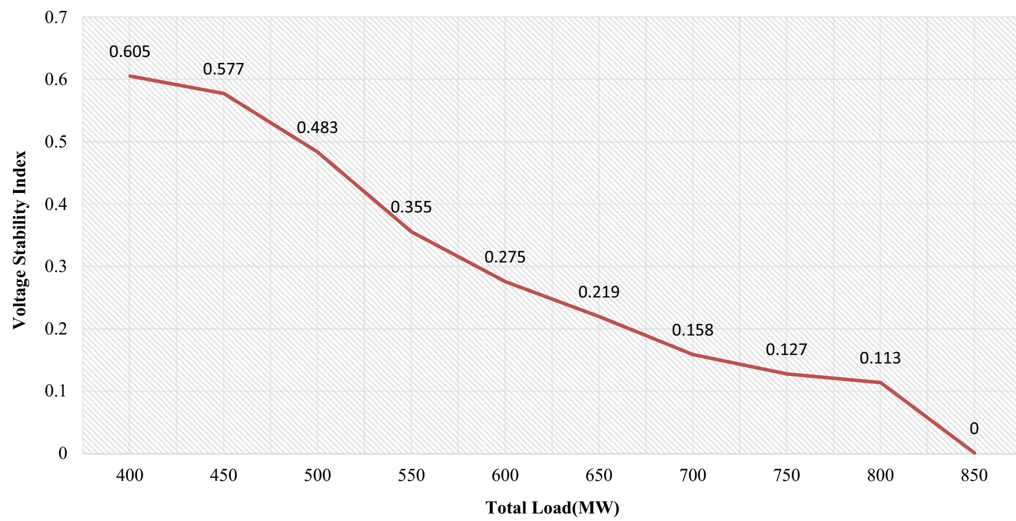


**Fig. 7** Variation in VSI for maximum load in WIS

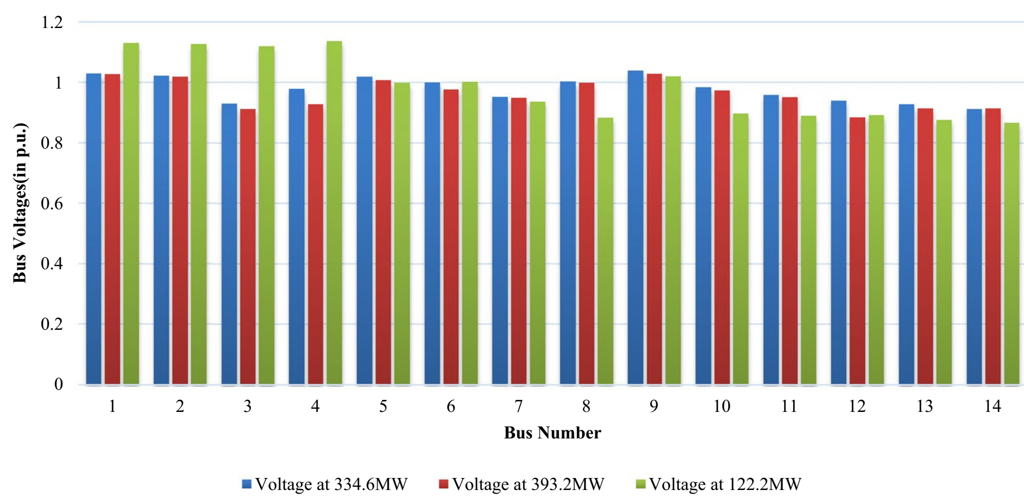


**Fig. 8** Voltage profile of buses using OPF with wind integration

**Table 3 Comparison of power loss with and without FACTS**

| S. no. | No of iterations | Load 400 (MW) | Load 300 (MW) | Load 150 (MW) | Total power loss (MW) WO FACT | Total power loss (MW) using SVC | Total power loss (MW) using TCSC |
|---|---|---|---|---|---|---|---|
| 1 | 0 | 400 | 300 | 150 | 15.16 | 14.69 | 15.55 |
| 2 | 1 | 440.68 | 299.12 | 125.77 | 15.78 | 14.63 | 15.60 |
| 3 | 2 | 433.94 | 300.11 | 131.74 | 15.84 | 14.60 | 15.46 |
| 4 | 3 | 435.87 | 299.94 | 130.42 | 15.83 | 14.60 | 15.42 |
| 5 | 4 | 434.13 | 299.99 | 130.71 | 15.83 | 14.32 | 15.44 |

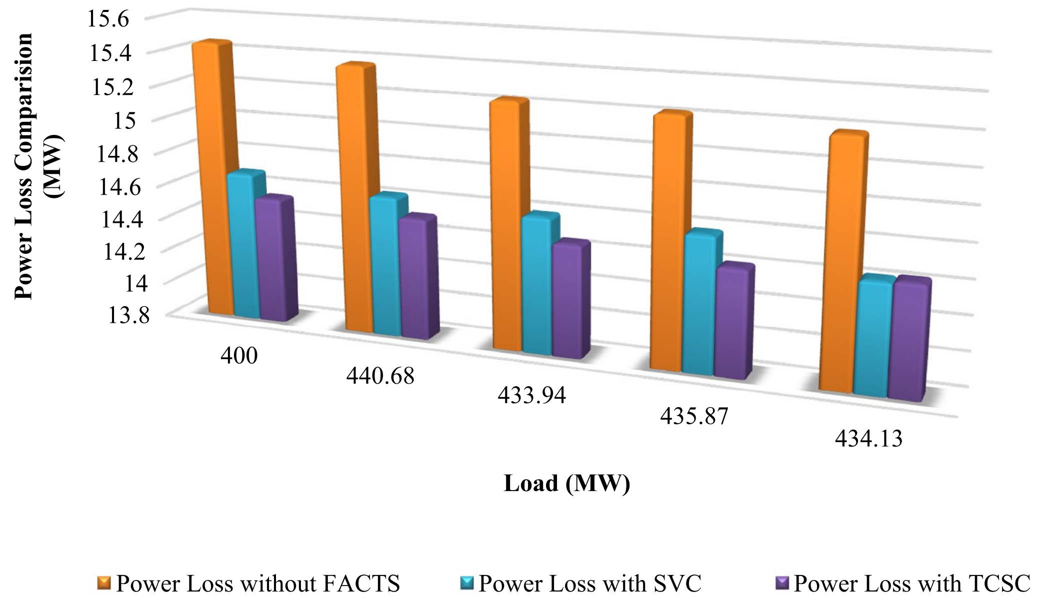


**Fig. 9** Comparison in power loss with and without FACTS

**Table 4 Voltage support by FACTS devices with firing controller for WIS**

| S. no. | Identified weak buses | Wind penetration level (%) | SVC firing angle control (°) | Voltage support by SVC (p.u.) | TCSC firing angle control (°) | Voltage support by TCSC (p.u.) |
|---|---|---|---|---|---|---|
| 1 | 1 | 20 | 138 | 0.5126 | 141.68 | 0.2865 |
| 2 | 12 | 40 | 129.31 | 0.3020 | 132.02 | 0.2327 |
| 3 | 11 | 50 | 131.59 | 0.2331 | 125.55 | 0.2119 |
| 4 | 13 | 75 | 130.27 | 0.2110 | 124.87 | 0.1985 |
| 5 | 14 | 100 | 130.60 | 0.2108 | 123.90 | 0.1888 |

**Table 5 Comparison of cost of power generation ($) per/50 MW/h with and without FACTS controllers**

| S. no. | Power generation (MW) | Cost of generation ($/h) without FACTS | Cost of generation ($/h) with SVC | Cost of generation ($/h) with TCSC |
|---|---|---|---|---|
| 1 | 150 | 723 | 658.5 | 640.5 |
| 2 | 200 | 964 | 878 | 854 |
| 3 | 250 | 1205 | 1097.5 | 1067.5 |
| 4 | 300 | 1446 | 1317 | 1281 |
| 5 | 350 | 1687 | 1536.5 | 1494.5 |
| 6 | 400 | 1928 | 1756 | 1708 |
| 7 | 450 | 2169 | 1975.5 | 1921.5 |
| 8 | 500 | 2410 | 2195 | 2135 |
| 9 | 550 | 2651 | 2414.5 | 2348.5 |
| 10 | 600 | 2892 | 2634 | 2562 |
| 11 | 650 | 3133 | 2853.5 | 2775.5 |
| 12 | 700 | 3374 | 3073 | 2989 |
| 13 | 750 | 3615 | 3292.5 | 3202.5 |
| 14 | 800 | 3856 | 3512 | 3416 |
| 15 | 850 | 4097 | 3731.5 | 3629.5 |

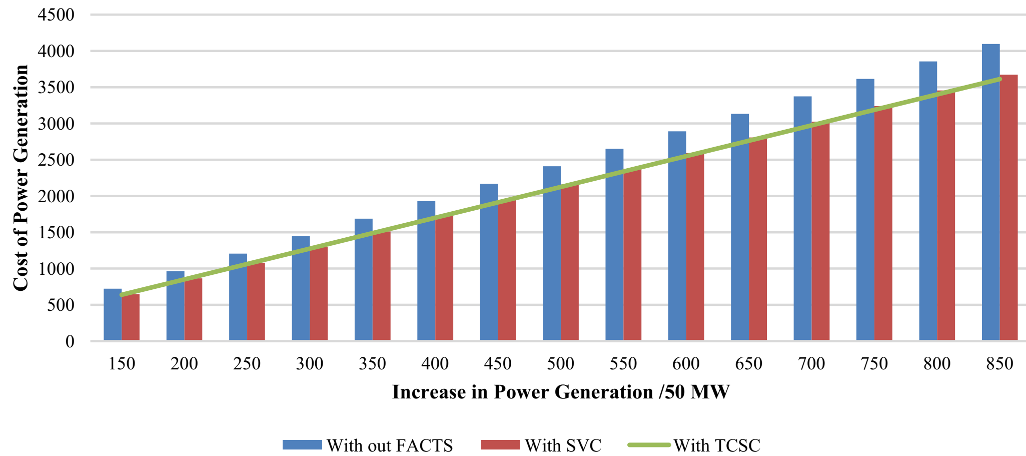


**Fig. 10** Saving in cost of generation with SVC and TCSC

artificial neural network; EP: evolutionary programming; DFIG: doubly fed induction generator; PSAT: power system analysis toolbox; VSI: voltage stability index; MW: megawatt; GAMS: general algebraic modelling system

## List of symbols

| | |
|---|---|
| $\rho$ | air density (kg/m$^3$) |
| $R$ | wind turbine rotor radius (m) |
| $V_\mathrm{w}$ | equivalent wind speed (m/s) |
| $\Theta$ | pitch angle of rotor |
| $C_\mathrm{P}$ | aerodynamics efficiency of rotor |
| $\lambda_w$ | tip speed ratio |
| $P_\mathrm{gn}$ | active power generation in the system by n no of units |
| $T_\mathrm{g}$ | total no of generators available in the system |
| $C_\mathrm{gn}$ | cost function of *n*th generator bus |
| $Q_k$ | reactive power of *k*th bus |
| $P_k$ | active power of *k*th bus |
| $X_C$ | capacitive reactance |
| $X_L$ | inductive reactance |
| $\alpha_\mathrm{SVC}$ | firing angle of static VAR compensator |
| $\Delta P_k$ | change in reactive power of *k*th bus at *i*th iteration |
| $\Delta Q_k$ | change in Active power of *k*th bus at *i*th iteration |
| $\lambda$ | change in the loading (variable load) condition of the wind-integrated system |
| $C_\mathrm{w}$ | operational wind power generation cost |
| $P_\mathrm{gw}$ | wind power generation cost |
| $C_n$ | operational conventional generation cost |
| $P_\mathrm{gn}$ | conventional generation output |
| $N_\mathrm{w}$ | number of weak buses in the system |
| $N_L$ | number of load buses in the system |
| $P_\mathrm{gn}^\mathrm{Min}$ | minimum active power limits of generators |
| $P_\mathrm{gn}^\mathrm{Max}$ | maximum active power limits of generators |
| $P_\mathrm{di}$ | active power demand at buses |
| $Q_\mathrm{di}$ | reactive power demand at buses |
| $Q_\mathrm{gn}^\mathrm{Min}$ | minimum reactive power limits of generators |
| $Q_\mathrm{gn}^\mathrm{Max}$ | maximum reactive power limits of generators |
| $Q_n$ | reactive power flow in the lines after placement of FACTS devices |
| $Q_{n-1}$ | reactive power flow in the lines before placement of FACTS devices |
| $V_n$ | node voltage of bus i |
| $V_n^\mathrm{Min}$ | minimum bus voltage |
| $V_n^\mathrm{Max}$ | maximum bus voltage |

### Authors' contributions

SK has simulated wind system with conventional IEEE 14 bus system with the use of PSAT and carried out preliminary sensitivity analysis for possibility of occurrence of fault. Modelling and optimization of FACTS devices are done by NKS. "Results and discussion" section was jointly drafted by SKC, AK and NKS. All the authors have read and approved the final manuscript.

### Authors' information

SKC was born in Mathura, U.P., India, in 1979. He received the B.Sc. Engineering degree in Electrical and Electronics Engineering from the Faculty of Engineering Dayalbagh Educational Institute, Dayalbagh Agra, U.P., India, in 2001, and M. Tech. in Electrical Engineering (Instrumentation & Control Engineering) from Aligarh Muslim University, AMU Aligarh, U.P., India, in 2004. Presently he is Ph.D student at National Institute of Technology (NITKKR), Kurukshetra, Haryana, India. His research area includes voltage stability, FACTS devices, optimization of renewable energy resources, performence and operation of renewable energy systems specially wind energy systems with economic operation of power system.


### Author details

[1] Department of Electrical Engineering, National Institute of Technology (NIT), Kurukshetra, Haryana 136119, India. [2] KIET Group of Institutions, Muradnagar, Ghaziabad, Uttar Pradesh 201206, India. [3] Department of Electrical Engineering, G L Bajaj Institute of Technology and Management, G B Nagar, Greater Noida, Uttar Pradesh 201306, India.

**Acknowledgements**
The author would like to thank and acknowledge Federico Milano, Associate Professor, School of Electrical and Electronic Engineering, University College Dublin, Belfield, Dublin 4, Ireland, for developing and providing a multipurpose PSAT software which has reduced the computational time and has made simulation of multimachine system very easy and user-friendly. The author would also like to acknowledge the Management and Department of EIE, KIET Group of Institution, Ghaziabad, for providing licensed version of the software and all necessary facilities for preparing this manuscript.

**Competing interests**
The authors declare that they have no competing interests.

## Appendix

### Bus data of IEEE 14 bus system

| Bus no. | P generated (p.u.) | Q generated (p.u.) | P load (p.u.) | Q load (p.u.) | Q generated max. (p.u.) | Q generated min. (p.u.) |
|---|---|---|---|---|---|---|
| 1 | 2.32 | 0.00 | 0.00 | 0.00 | 10.0 | −10.0 |
| 2 | 0.4 | −0.424 | 0.2170 | 0.1270 | 0.5 | −0.4 |
| 3 | 0.00 | 0.00 | 0.9420 | 0.1900 | 0.4 | 0.00 |
| 4 | 0.00 | 0.00 | 0.4780 | 0.00 | 0.00 | 0.00 |
| 5 | 0.00 | 0.00 | 0.0760 | 0.0160 | 0.00 | 0.00 |
| 6 | 0.00 | 0.00 | 0.1120 | 0.0750 | 0.24 | −0.06 |
| 7 | 0.00 | 0.00 | 0.00 | 0.00 | 0.00 | 0.00 |
| 8 | 0.00 | 0.00 | 0.00 | 0.00 | 0.24 | −0.06 |
| 9 | 0.00 | 0.00 | 0.2950 | 0.1660 | 0.00 | 0.00 |
| 10 | 0.00 | 0.00 | 0.0900 | 0.0580 | 0.00 | 0.00 |
| 11 | 0.00 | 0.00 | 0.0350 | 0.0180 | 0.00 | 0.00 |
| 12 | 0.00 | 0.00 | 0.0610 | 0.0160 | 0.00 | 0.00 |
| 13 | 0.00 | 0.00 | 0.1350 | 0.0580 | 0.00 | 0.00 |
| 14 | 0.00 | 0.00 | 0.1490 | 0.5000 | 0.00 | 0.00 |

### Load flow for IEEE 14 bus system

| Bus | Voltage (p.u.) | Phase (radian) | P gen. (p.u.) | Q gen. (p.u.) | P load (p.u.) | Q load (p.u.) |
|---|---|---|---|---|---|---|
| Bus 1 | 1.06 | 0 | 7.7641 | 2.3902 | 0.0 | 0.0 |
| Bus 2 | 0.9313 | −0.3140 | −0.1019 | 1.7701 | 0.5147 | 0.3012 |
| Bus 3 | 0.8726 | −0.7998 | 0.01975 | 1.6899 | 2.2343 | 0.4506 |
| Bus 4 | 0.7991 | −0.6182 | 0.0 | 0.0 | 1.1338 | 0.0948 |
| Bus 5 | 0.8118 | −0.5168 | 0.0 | 0.0 | 0.1802 | 0.0379 |
| Bus 6 | 0.8624 | −0.9064 | 0.01794 | 0.8872 | 0.2656 | 0.1778 |
| Bus 7 | 0.8428 | −0.8273 | 0.0 | 0.9179 | 0.0 | 0.0 |
| Bus 8 | 1.0039 | −0.8302 | 0.01403 | 0.0 | 0.0 | 0.0 |
| Bus 9 | 0.7702 | −0.9410 | 0.0 | 0.0 | 0.6997 | 0.3937 |
| Bus 10 | 0.7621 | −0.9556 | 0.0 | 0.0 | 0.2134 | 0.1375 |
| Bus 11 | 0.8004 | −0.9385 | 0.0 | 0.0 | 0.0830 | 0.0426 |
| Bus 12 | 0.8106 | −0.9644 | 0.0 | 0.0 | 0.1446 | 0.0379 |
| Bus 13 | 0.7906 | −0.9685 | 0.0 | 0.0 | 0.3202 | 0.1375 |
| Bus 14 | 0.7153 | −1.0341 | 0.0 | 0.0 | 0.3534 | 0.1185 |

## Numerical data

### Line flows for IEEE 14-bus test system

| From bus | To bus | Line | P flow (p.u.) | Q flow (p.u.) | P loss (p.u.) | Q loss (p.u.) |
|---|---|---|---|---|---|---|
| Bus 02 | Bus 05 | 1 | 1.0068 | 0.3848 | 0.0770 | 0.2092 |
| Bus 06 | Bus 12 | 2 | 0.1986 | 0.0838 | 0.0076 | 0.0159 |
| Bus 12 | Bus 13 | 3 | 0.0462 | 0.0299 | 0.0010 | 0.0009 |
| Bus 06 | Bus 13 | 4 | 0.4540 | 0.2546 | 0.0241 | 0.0474 |
| Bus 06 | Bus 11 | 5 | 0.1958 | 0.1777 | 0.0089 | 0.0186 |
| Bus 11 | Bus 10 | 6 | 0.1039 | 0.1156 | 0.0031 | 0.0072 |
| Bus 09 | Bus 10 | 7 | 0.1134 | 0.0311 | 0.0007 | 0.0019 |
| Bus 09 | Bus 14 | 8 | 0.2187 | 0.0623 | 0.0110 | 0.0235 |
| Bus 14 | Bus 13 | 9 | −1.4570 | −0.0791 | 0.0092 | 0.0187 |
| Bus 07 | Bus 09 | 10 | 0.6697 | 0.5949 | 0.0 | 0.1242 |
| Bus 01 | Bus 02 | 11 | 5.5780 | 1.2648 | 0.5655 | 1.6741 |
| Bus 03 | Bus 02 | 12 | −1.766 | 0.6187 | 0.2173 | 0.8799 |
| Bus 03 | Bus 04 | 13 | −0.4881 | 0.6204 | 0.0562 | 0.1194 |
| Bus 01 | Bus 05 | 14 | 2.1862 | 1.1262 | 0.2938 | 1.1691 |
| Bus 05 | Bus 04 | 15 | 1.5098 | −0.1584 | 0.0466 | 0.1388 |
| Bus 02 | Bus 04 | 16 | 1.4056 | 0.4128 | 0.1446 | 0.4108 |
| Bus 05 | Bus 06 | 17 | 1.1321 | 0.2531 | 0.0 | 0.4469 |
| Bus 04 | Bus 09 | 18 | 0.3628 | 0.1397 | 0.0 | 0.1233 |
| Bus 04 | Bus 07 | 19 | 0.6836 | −0.0290 | 0.0 | 0.1466 |
| Bus 08 | Bus 07 | 20 | 0.01403 | 0.9179 | 0.0 | 0.1472 |

### Line data for IEEE 14-bus test system

| From bus | To bus | Resistance (p.u.) | Reactance (p.u.) | Line charging (p.u.) | Tap ratio |
|---|---|---|---|---|---|
| 1 | 2 | 0.0193 | 0.0591 | 0.0528 | 1 |
| 1 | 5 | 0.0540 | 0.2230 | 0.0492 | 1 |
| 2 | 3 | 0.0469 | 0.1979 | 0.0438 | 1 |
| 2 | 4 | 0.0581 | 0.1763 | 0.034 | 1 |
| 2 | 5 | 0.0569 | 0.1738 | 0.0346 | 1 |
| 3 | 4 | 0.0670 | 0.1710 | 0.0128 | 1 |
| 4 | 5 | 0.0133 | 0.0421 | 0.0128 | 1 |
| 4 | 7 | 0.00 | 0.2091 | 0.00 | 0.978 |
| 4 | 9 | 0.00 | 0.5561 | 0.00 | 0.969 |
| 5 | 6 | 0.00 | 0.2520 | 0.00 | 0.932 |
| 6 | 11 | 0.0949 | 0.1989 | 0.00 | 1 |
| 6 | 12 | 0.1229 | 0.2558 | 0.00 | 1 |
| 6 | 13 | 0.0661 | 0.1302 | 0.00 | 1 |
| 7 | 8 | 0.00 | 0.1761 | 0.00 | 1 |
| 7 | 9 | 0.00 | 0.1100 | 0.00 | 1 |
| 9 | 10 | 0.0318 | 0.0845 | 0.00 | 1 |
| 9 | 14 | 0.1271 | 0.2703 | 0.00 | 1 |
| 10 | 11 | 0.0820 | 0.1920 | 0.00 | 1 |
| 12 | 13 | 0.2209 | 0.1998 | 0.00 | 1 |
| 13 | 14 | 0.1709 | 0.3480 | 0.00 | 1 |

**Generator cost coefficient**

| $a_n$ (\$/MW h)$^2$) | $b_n$ (\$/MW h) | $c_n$ (\$/h) |
|---|---|---|
| 0.00375 | 2.00 | 95 |
| 0.01750 | 1.75 | 30 |
| 0.06250 | 1.00 | 45 |
| 0.00834 | 3.25 | 55 |
| 0.02500 | 3.00 | 65 |

Received: 15 September 2016 Accepted: 7 February 2017
Published online: 07 March 2017

**References**

Ajjarapu, V., & Christy, C. (1998). The continuous power flow: A tool for steady state voltage stability analysis. *IEEE Transaction on Power System, 13*(1), 417–423.

Al Rashidi, M. R., Al Hajri, M. F., & El Naggar, K. M. (2010). Particle swarm optimization and its applications in power systems. *Computational Intelligence in Power Engineering, SCI, 302,* 295–324.

Chi, Y., Liu, Y., Wang, W., & Dai, H. (2006). Voltage stability analysis of wind system. In *Integration into transmission network, international conference on power system technology* (pp. 1–7).

Ehtesham, R., Khatoon, S., & Naseeruddin, I. (2016). Optimal and suboptimal controller design for wind power system. *Renewables Wind, Water, and Solar, 3*(1), 1–12.

Gaddada, S., & Kodicherla, S. P. K. (2016). Wind energy potential and cost estimation of wind energy conversion systems (WECSs) for electricity generation in the eight selected locations of Tigray region (Ethiopia). *Renewables: Wind, Water, and Solar, 10*(3), 1–13.

Gerbex, S., Cherkaoui, R., & Germond, A. J. (2001). Optimal location of multi-type FACTS devices by means of genetic algorithm. *IEEE Transaction on Power System, 16*(3), 537–544.

Hetzer, J., Yu, D. C., & Bhattarai, K. (2008). An economic dispatch model incorporating wind power. *IEEE Transaction in Energy Conversion, 23*(2), 603–611.

Ilic, M., & Stankovic, A. (1991). Voltage problems on transmission networks subjected to unusual power flow patterns. *IEEE Transaction on Power System, 6*(1), 339–348.

Joslin Hurbert, G., Miniyan, S., Srivalasan, E., & Rajapandian, S. (2007). A review of wind energy technology. *Renewable and Sustainable Energy Review, 11*(6), 1117–1145.

Jovcic, D., & Pillai, G. N. (2005). Analytical modelling of TCSC dynamics. *IEEE Transactions on Power Delivery, 20*(2), 1097–1104.

Lof, P. A., Anderson, G., & Hill, D. J. (1992).Voltage stability indices for stressed power systems. In *IEEE PES winter meeting*, New York (pp. 326–335).

Mo, N., Zou, Z. Y., Chan, K. W., & Pong, T. Y. G. (2007). Transient stability constrained optimal power flow using particle swarm optimization. *IET Generation, Transmission and Distribution, 1*(3), 476–483.

Momoh, J. A. (1989). Optimal power flow with multiple objective function. In *Power symposium 1989, proceedings of 21st annual North-America* (pp. 105–108).

Momoh, J. A. (2001). *Electric power system applications of optimization* (2nd ed.). Spain: CRC Press.

Momoh, J. A., Koessler, R. J., Bond, M. S., Scott, B., Sun, D., & Papalexopoulos, A. (1997). Challenges to optimal power flow. *IEEE Transactions on Power systems, 12*(1), 444–455.

Musirin, I., Khawa, T., & Rahman, A. (2002) Novel fast voltage stability indices (FVSI) for voltage stability analysis in power transmission system. In *Student conference on research and development proceedings*, SCORED-2002, Shah Alam Malaysia (Vol. 2, No. 5, pp. 265–268).

Prasanthi, A., & Sindhu, T. K. (2014). Optimal placement and rating of FACTS devices for congestion Management in power system without and with wind energy integration. In *IEEE international conference on advanced communication control and computing technologies (ICACCCT)* (pp. 224–229).

Reis, C., & Maciel Barbosa, F. P. (2009). Line indices for voltage stability assessment. In *Power-tech conference*, 28 June–2 July Bucharest, Romania (pp. 1–6).

Saravanan, M., Raja Slochanal, S. M., Venkatesh, P., & Prince Stephen Abraham, J. (2007). Application of particle swarm optimization technique for optimal location of FACTS devices considering cost of installation and system loadability. *Electric Power Systems Research, 77*(3), 276–283.

Segura, I., Escriva, G., & Alcazar-Ortega, M. (2011). Wind system electrical power production modal for load flow analysis. *Elsevier Renewable Energy, 36*(2), 1008–1013.

Shakib, A. D., Spahic, E., & Balzer, G. (2009). Optimal location of series FACTS devices to control line over loads in power systems with high wind feeding. In *IEEE Bucharest power tech conference, June 28th–July 2nd,* Bucharest, Romania (pp. 1–7).

Sharma, A. K., Mittapalli, R. K., & Pal, Y. (2016). FACTS devices cost recovery during congestion management in deregulated electricity markets. *Journal of Institute of Engineers India Series-B, 97*(3), 339–354.

Shi, L., Wang, C., Yao, L., Ni, Y., & Bazargan, M. (2012). Optimal power flow solution incorporating wind power. *IEEE Systems Journal, 6*(2), 233–241.

Venkatesh, P., Gnanadass, R., & Padhy, N. P. (2003). Comparison and application of evolutionary programming techniques to combined economic emission dispatch with line flow constraints. *IEEE Transaction on Power System, 18*(2), 688–697.

Wood, A. J., & Wollenberg, B. F. (1996). *Power generation, operation, and control*. New York, NY: Wiley.

Yuryevich, J., & Wong, K. P. (1999). Evolutionary programming based optimal power flow algorithm. *IEEE Transaction on Power Systems, 14*(4), 1245–1250.

Zimmerman, R., Murillo-Sanchez, E., & Gan, D. (2007). MATPOWER: MATLAB Power System Simulation Package.